

RSC Advances



This is an *Accepted Manuscript*, which has been through the Royal Society of Chemistry peer review process and has been accepted for publication.

Accepted Manuscripts are published online shortly after acceptance, before technical editing, formatting and proof reading. Using this free service, authors can make their results available to the community, in citable form, before we publish the edited article. This *Accepted Manuscript* will be replaced by the edited, formatted and paginated article as soon as this is available.

You can find more information about *Accepted Manuscripts* in the [Information for Authors](#).

Please note that technical editing may introduce minor changes to the text and/or graphics, which may alter content. The journal's standard [Terms & Conditions](#) and the [Ethical guidelines](#) still apply. In no event shall the Royal Society of Chemistry be held responsible for any errors or omissions in this *Accepted Manuscript* or any consequences arising from the use of any information it contains.

Synthesis of higher alcohols by Fischer-Tropsch reaction over activated
carbon supported CoCuMn catalysts

Yanpeng Pei^{a,*}, Siping Jian^b, Yuanyuan Chen^a, Chuncheng Wang^a

^a *Guangzhou Pysynchem. Co. Ltd., Guangzhou 510640, China*

^b *School of Chemistry and Chemical Engineering, South China University
of Technology, Guangzhou 510640, China*

Abstract

Activated carbon supported CoCuMn catalysts prepared by incipient co-impregnation were studied by using Fischer-Tropsch reaction, XRD, HR-TEM, and H₂-TPR techniques. The results showed that good activities and selectivities towards C₁-C₁₄ alcohols can be obtained with the fractions of C₂-C₅ alcohols up to 80% in total alcohols. It is found that increasing the Cu/Co composition ratio resulted in the enhancement of alcohol selectivity. Furthermore, our characterizations revealed that large Cu nano-particles were decorated by small, spherical Co nano-particles, which we speculate that such construction were responsible for the favored formation of C₂₊ alcohols. It is also considered that smaller cobalt particles probably resulted in more number of Co⁰ and thus contributed to the improvement of CO conversion.

Keywords: Higher alcohol; Fischer-Tropsch reaction; CoCuMn;

Introduction

The Fischer-Tropsch (FT) synthesis, which produces hydrocarbons

with oxy-compounds as byproducts from coal, natural gas and biomass via syngas intermediate, has long been known and has received renewed attentions in recent years due to environmental concerns and energy issues, because the products i.e. hydrocarbons and oxy-compounds can serve as alternative fuels and valuable chemical feedstock to petroleum refining [1]. Many transitional metals such as Fe, Co, Ni, and Ru can be used as catalysts for FT synthesis [2,3]. Among these catalysts, supported Co catalysts appear as one of the most promising candidates for FT synthesis because of their workable cost, high FT activity, high selectivity towards long-chain hydrocarbons and low water gas shift activity [1,4]. It is well recognized that the active site for CO dissociation, carbon chain growth and hydrocarbon formation is metallic Co phase, whereas the production of alcohols usually requires synergy between proximate catalytic sites as both the dissociative sites and the non-dissociative insertion of CO. For instance, dual metal catalysts such as CuCo, CuFe and RuMo based catalysts have been regarded as materials capable of providing the necessary synergic actions [5,6].

Recently, one-pot production of long chain α -alcohols (i.e. alcohols with carbon number larger than six) via FT reaction over Co-based catalysts has aroused particular interest, owing to that these products are used as intermediates in the synthesis of plasticizers, detergents and lubricants. For instance, Xiang et al. reported that ternary “CoCuMn”

metal catalysts could be tuned to strongly favor product of straight C₁-C₁₄ terminal alcohols [7,8]. Alkali metals modified unsupported and SiO₂ supported Co catalysts have been reported to be selective for the production of C₁-C₁₆ alcohols as well [9]. However, high alcohol selectivity was achieved at the expense of activity for the former case while there was very high CO₂ selectivity for the latter case. In a previous study, activated carbon (AC) supported Co (Co/AC) catalysts have been reported to be able to produce C₁-C₁₈ linear alcohols in the presence of Co and in situ formed Co₂C phases, which were supposed to play a pivotal role in alcohol formation during FT reaction. It is further revealed that addition of La₂O₃ into the Co/AC catalysts could provide additional site for alcohol formation and thereby improved alcohol selectivity [10]. Also, to increase the activity of Co/AC catalysts, methods to decrease the size of Co particles are suggested to be adopted [11]. More importantly, it is demonstrated that the Co/AC catalysts have many inherent advantages, such as that the catalysts are tunable to increase alcohol selectivity and activity simultaneously, and to generate low production of methane, CO₂ and methanol [10-12]. These results indicate that the Co/AC catalysts appear to be promising candidates for further modification to meet the necessity for large-scale industrial production of higher alcohols.

In the present study, we reported a study of AC supported CoCuMn (CoCuMn/AC) catalysts for the synthesis of higher alcohols from syngas

via FT reaction under the consideration listed as follows. (1) AC supported Co catalysts can be anticipated to produce alcohols with little methanol fractions; (2) Cu metal can serve as a site in favor of the production of alcohols; (3) Mn species were introduced into the as-prepared catalysts as a promoter to improve catalyst performance. The performance data of all the catalysts were correlated with the results of TPR, XRD and HR-TEM characterizations.

Experimental

Catalyst preparation

AC made from coconut shells was purchased from Tangshan Union Activated Carbon Co. Ltd.. Before use, the material was washed with de-ionized water for several times to eliminate the mineral impurities [13], followed by crushed into 80-100 meshes. A Co/AC catalyst used for reference was prepared by the incipient wetness impregnation of AC with an aqueous solution of cobalt nitrate (Sinopharm Chemical Reagent Co. Ltd.). The wet sample was dried at 333 K for 6 h in air and finally calcined at 523 K for 4 h under pure Ar. The obtained catalyst was denoted as 15Co. CoCuMn/AC catalysts were prepared by impregnating the AC with mixed solution of cobalt, cupric, and manganous nitrate (Sinopharm Chemical Reagent Co. Ltd.), dried and calcined under the same conditions as mentioned above. The obtained catalysts were denoted here as 15Co4Cu4Mn, 15Co8Cu8Mn and 8Co8Cu8Mn, respectively. For

comparison, an AC supported CoCu bi-metal catalyst was prepared using the same procedure as described above after impregnating the AC with mixed solution of cobalt and cupric nitrate (Sinopharm Chemical Reagent Co. Ltd.), and denoted as 15Co4Cu. The numbers adopted for catalyst nomenclature indicate the mass percentages of each metal component behind them relative to the initial mass of the support material in the dried catalyst.

Catalytic test

A fixed bed reactor was used for FT synthesis. Catalysts (4 ml, diluted with quartz sand to a volume ratio of 1:1) were in situ pretreated in a flow of H₂ (60 ml/min) at 703 K for 4 h at normal pressure. After the catalysts were cooled to room temperature, the reactor was purged with syngas (H₂/CO = 2:1) and then charged with syngas at 3.0 MPa and a flow rate of 500 h⁻¹, and the temperature was increased at a 0.3 K/min heating rate to 493 K. The reaction effluent passed through a condenser to collect the liquid products. The moment when the reactor reached the designed temperature was taken as starting time. After 24 h stabilization, the liquid organic products and the aqueous products for another 24 h were off-line analyzed on HP-6890 GC with 5% PH ME capillary columns and FID detector after being carefully separated. The outlet gas was on-line analyzed by HP-6890 GC with a Parapack-Q column and TCD detector.

Catalyst characterization

The crystalline phases of catalysts after reduction and reaction were examined by X-ray diffraction (XRD) with Cu $K\alpha_1$ radiation on a PANalytical X'Pert PRO diffractometer at 40 kV and 40 mA. The spectra were recorded from 20 to 60° at a scanning rate of 10°/min. For the measurements, the catalysts were ground to fine powder and placed inside a dish.

H₂-TPR experiments were carried out on an Altamira Instruments temperature programmed system (AMI-200). The sample (50 mg) was treated by a 10% H₂/Ar gas mixture in a flow rate of 50 ml/min, and the reduction temperature was increased from room temperature to 1123 K at a heating rate of 10 K/min. The hydrogen consumption was recorded online with a mass spectrometer (MS) (Oministar, Pfeiffer Vacuum).

The morphology and crystalline nature of the samples were studied by high-resolution transmission electron microscopy (HR-TEM, C/M300 from Philips), operating at 300 kV. A few droplets of a suspension of the calcined catalysts in ethanol were put on a micro-grid carbon polymer supported on a copper grid and allowed to dry at room temperature for HR-TEM observations.

3. Results and discussion

3.1. The performance of FT reaction

Table 1 shows the results of catalytic tests for the 15Co catalyst and the CoCuMn/AC catalysts in terms of CO conversion, selectivity and

alcohol distribution. It is seen that the activity (CO conversion) significantly increased when 4% Cu and 4% Mn were added into the 15Co catalyst. A further increase of Cu and Mn with equal contents only results in a slight increase in activity. It is interesting to observe that the activity was still enhanced when the loading of Co was reduced with the loading of Cu and Mn keeping the maximum value. The CH₄ selectivities showed an opposite trend to the activity. The selectivities for the formation of C₂-C₄ hydrocarbons remain almost unchanged for all the catalysts. The selectivity towards CO₂ formation on the 15Co4Cu4Mn, 15Co8Cu8Mn, and 8Co8Cu8Mn catalysts were slightly higher than that of the 15Co catalyst, which can be attributed to the addition of copper that enhances the water gas shift reaction. The selectivities of C₅+ hydrocarbon significantly increases as 4% Cu and 4% Mn were added into the 15Co catalyst and then decreased to lowest in the sequence of the 15Co8Cu8Mn and 8Co8Cu8Mn catalysts. All catalysts produce alcohols, among which the 15Co catalyst showed the lowest selectivity to alcohols but exhibited a minor increase in alcohol selectivity when 4% Cu and 4% Mn were added. When the content of Cu and Mn were doubled, the selectivity to alcohols ramped up slowly, however, a significant increase in alcohol selectivity can be observed when the loading of Co were reduced to 8% with the content of Cu and Mn keeping doubled. The fraction of methanol and C₆-C₁₄ alcohols decreased while that of C₂-C₅

alcohols increased in the sequence of the 15Co, 15Co4Cu4Mn, 15Co8Cu8Mn and 8Co8Cu8Mn catalysts, which indicated that the addition of Cu and Mn favored to confine the formation of alcohols in the carbon number range of 2 to 5.

Table 1 Performance of FT reaction over the 15Co catalyst and the CoCuMn/AC catalysts^a.

Catalyst	CO conv. (C%)	Selectivity (C%)				Alcohol distribution (C%)			
		CH ₄	C ₂ -C ₄ ^b	CO ₂	C ₅₊ ^c	Total alcohols	MeOH ^d	C ₂ -C ₅ OH ^e	C ₆ -C ₁₄ OH ^f
15Co	34.6	32.0	21.9	0.9	25.1	20.1	10.1	47.1	42.8
15Co4Cu4Mn	52.2	14.1	22.0	3.8	36.6	23.5	6.6	54.2	39.2
15Co8Cu8Mn	56.0	8.9	26.1	5.9	34.1	25.0	3.1	68.5	28.4
8Co8Cu8Mn	58.3	7.7	22.5	5.2	24.5	40.1	2.7	80.0	17.3

^a Reaction conditions: P = 3.0 MPa, GHSV = 500 h⁻¹, T = 493 K.

^b Hydrocarbons with carbon numbers from 2-4.

^c Hydrocarbons with carbon numbers more than 4.

^d Methanol.

^e Alcohols with carbon numbers of 2-5.

^f Alcohols with carbon numbers of 6-14.

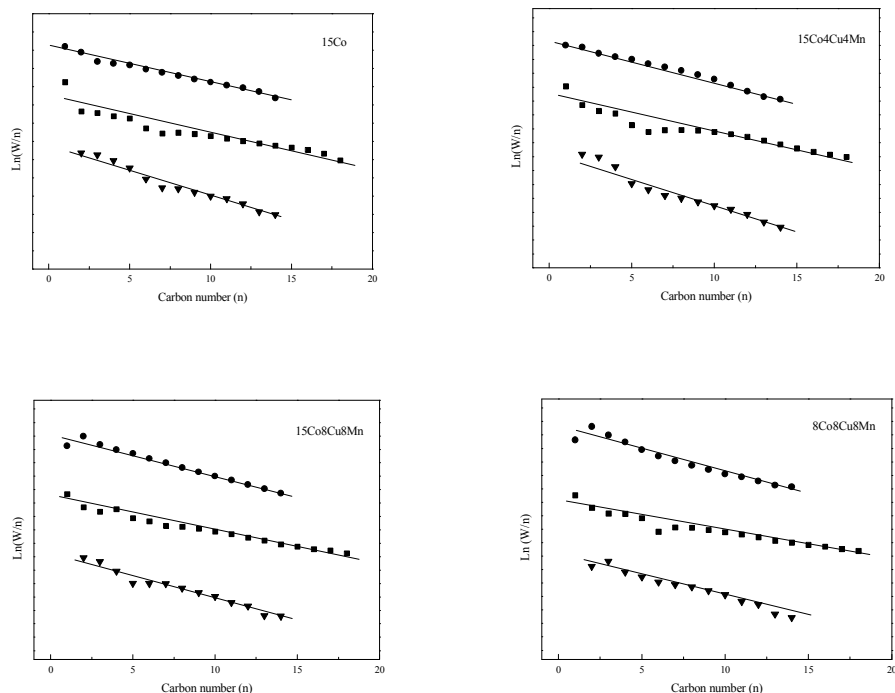


Fig. 1 The ASF product distribution of the 15Co and the CoCuMn/AC catalysts: (●) Alcohol (■) Paraffin (▼) Olefin.

The Anderson-Schulz-Flory (ASF) product distributions for the formation of alcohols, olefins and paraffins over the 15Co and the CoCuMn/AC catalysts are presented in Fig.1 (showing data for alcohols and olefins up to C₁₄ and paraffins up to C₁₈). There are slight deviations in the case of paraffins with fewer than nine carbons (such as methane and heptane), olefins with fewer than seven carbons (such as ethylene and hexene), and alcohols with one or two carbons that we believe may be ascribed to an acceptable level of experimental error. Generally, though, the product distributions all generated linear ASF plots. This indicates a chain growth mechanism by successive addition of a C₁ species in the insertion process as previously proposed for the chain growth in the literature [14]. Table 2 lists the chain-growth probability factors (α) for paraffin, olefin and alcohol products. The α values for alcohols are seen to be decreased while those of paraffins remain almost constant, whereas those for olefins increased slightly in the sequence of the 15Co, 15Co4Cu4Mn, 15Co8Cu8Mn, 8Co8Cu8Mn catalysts. This result again demonstrated that short-chain alcohols are favorably produced when Cu and Mn are doped into the 15Co catalyst.

Table 2 Chain growth probability factors of alcohols, paraffins, and olefins of the 15Co and the CoCuMn/AC catalysts.

	catalysts			
	15Co	15Co4Cu4Mn	15Co8Cu8Mn	8Co8Cu8Mn
α_{alcohols}	0.67	0.63	0.62	0.60
$\alpha_{\text{paraffins}}$	0.67	0.71	0.67	0.71
α_{olefins}	0.59	0.59	0.64	0.66

3.2. TPR results

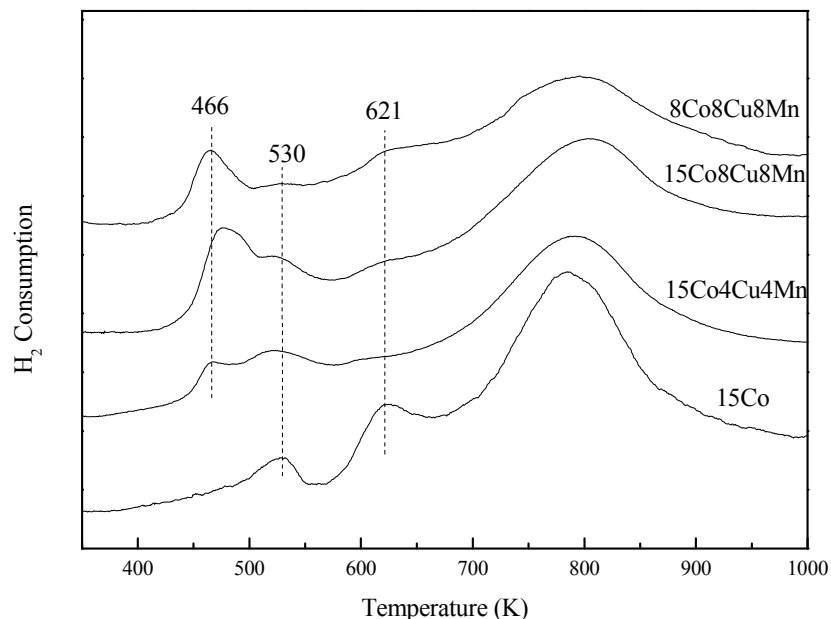


Fig. 2 TPR profiles of the 15Co and the various CoCuMn/AC catalysts.

TPR experiments were carried out under flowing H₂/Ar to investigate catalyst reducibility for the 15Co and the CoCuMn/AC catalysts, and the results were displayed in Fig. 2. There were three reduction peaks at 530, 621 and above 700 K for the 15Co catalyst. The broad peak above 700 K could be assigned to hydrogenation of surface oxygen-containing groups on the AC support in the presence of Co metal [15,16], while the other two reduction peaks corresponded to a consecutive reduction of Co₃O₄ through CoO to Co⁰ [10,17,18]. Besides the above-mentioned peaks, a new peak at ca. 466 K can be clearly observed on the 15Co4Cu4Mn, 15Co8Cu8Mn and 8Co8Cu8Mn catalysts.

It is shown by XRD characterization results (see the following section) that metallic Cu phases were clearly present on the three catalysts after reduction while it is also reported that copper ions can be easily reduced to metallic copper at temperature below 523 K [19]. Thus, it is reasonable to attribute this new peak to the reduction of Cu^{2+} to metallic Cu. The peak position of Co_3O_4 to CoO and CoO to Co reduction was almost the same on all the catalysts, indicating that the addition of Cu and Mn species did not alter the interaction of Co species with the support. However, the area of CoO to Co reduction peak suddenly reduced when 4% Cu and 4% Mn components were added into the 15Co catalyst, and then gradually increased in the sequence of the 15Co4Cu4Mn, 15Co8Cu8Mn and 8Co8Cu8Mn catalysts. The areas of the CoO to Co reduction peak on the 15Co4Cu4Mn, 15Co8Cu8Mn and 8Co8Cu8Mn catalysts were much smaller than that on the 15Co catalysts, which indicated that the three catalysts had decreased reducibility as compared to the 15Co catalyst. No peaks corresponding to the reduction of Mn species were identified during TPR process. Thus, Mn species did not reduce to a metallic state, which is in agreement with what the literature reports [20,21].

3.3. XRD results

XRD patterns for the 15Co and the CoCuMn/AC catalysts after reduction and subsequent passivation were shown in Fig. 3. The 15Co catalyst showed only one small peak at $2\theta = 44.3^\circ$, which could be

attributed to metallic Co (PDF 00-001-1259). For the three reduced CoCuMn/AC catalysts, one can see that besides the metallic Co peak, new peaks at $2\theta = 43.4$ and 50.3° appeared, which could be assigned to metallic Cu (PDF 00-001-1241). The intensities of Cu peaks increased while the intensity of the Co peak decreased in the sequence of 15Co, 15Co4Cu4Mn, 15Co8Cu8Mn and 8Co8Cu8Mn catalysts. This indicated that large Cu particles and small Co are willing to form according to the above tendency. Powder X-ray diffraction patterns elucidate the co-existence of distinctive fundamental peaks for both Co and Cu, indicating that they have not formed an alloy during the reduction process. This is in consistence with the findings that Co and Cu metals do not alloy [22-24]. No apparent peaks ascribed to manganese-containing species can be found, indicating that they were probably quite finely dispersed on the surface of the activated carbon support.

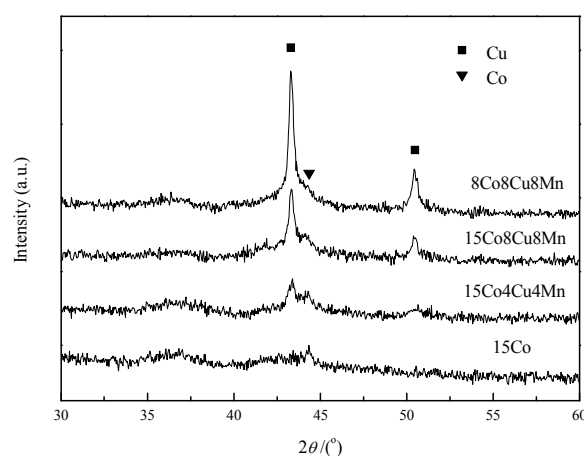


Fig. 3: Powder XRD patterns for the 15Co and the CoCuMn/AC catalysts after reduction and subsequent passivation.

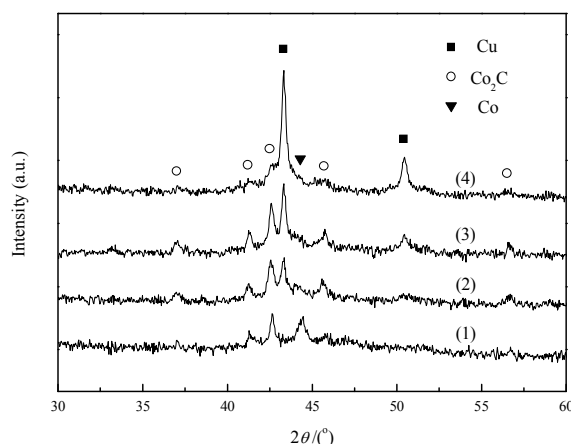


Fig. 4 XRD patterns of the 15Co and the CoCuMn/AC catalysts after reaction and subsequent passivation: (1) 15Co; (2) 15Co4Cu4Mn; (3) 15Co8Cu8Mn; (4) 8Co8Cu8Mn.

Fig.4 showed the XRD patterns of the 15Co and the CoCuMn/AC catalysts after reaction and subsequent passivation. For the used 15Co catalyst, besides a characteristic peak of metallic Co (at $2\theta = 44.3^\circ$), new peaks (at $2\theta = 37.0^\circ$, 41.2° , 42.5° , 45.7° and 56.6°) belonging to Co_2C (PDF 01-072-1369) can be observed, which indicated that Co_2C species were formed during reaction. Similar phenomena were observed over Co/AC catalysts in the literature [10]. For the used 15Co4Cu4Mn, 15Co8Cu8Mn and 8Co8Cu8Mn catalysts, characteristic peaks of metallic Co, Co_2C and metallic Cu could be identified simultaneously, indicating their co-existence in the specific sample. The intensities of Co_2C peaks slightly increased in the sequence of the 15Co, 15Co4Cu4Mn and 15Co8Cu8Mn catalysts, but became very weak for the 8Co8Cu8Mn catalyst. This indicated that the formation of Co_2C was promoted on the 15Co4Cu4Mn and 15Co8Cu8Mn catalysts, but inhibited on the

8Co8Cu8Mn catalyst, as compared with the 15Co catalyst, which indicated that there were probably not enough Co species available for the formation of Co_2C on the 8Co8Cu8Mn catalyst as compared with the other three catalysts when Co loadings were reduced. Alternately, there is probably a dynamic balance between in situ formed Co and Co_2C phases on Co/AC catalysts during reaction, which can be influenced by several factors such as promoters or Co loadings. In fact, it is reported in the literatures that many factors are capable of affecting the formation of Co_2C on Co/AC catalysts, such as the presence of promoters [10], variations in Co particle sizes [11], and/or reaction temperature [25], but a more thorough analysis is still necessary, which is not the aim of the present work. The XRD patterns of Cu on the spent 15Co4Cu4Mn, 15Co8Cu8Mn and 8Co8Cu8Mn catalysts were almost the same as those on the corresponding reduced catalysts aside from very slight increase in intensities, which indicated that no apparent structure change or particle aggregation of Cu species occurred. The intensity of Co^0 on the used 15Co catalyst was very strong as compared with that on the reduced catalyst, indicating significant Co aggregation occurred. The spent 15Co4Cu4Mn, 15Co8Cu8Mn and 8Co8Cu8Mn catalysts showed only weak XRD peaks of metallic Co, which is an indication that small particles of Co were formed on these catalysts. The intensities of the Co peaks decreased in the sequence of 15Co4Cu4Mn, 15Co8Cu8Mn and

8Co8Cu8Mn catalysts, which indicated that the Co particle size decreased in the same trend. Additionally, the intensities of metallic Co on the spent 15Co4Cu4Mn, 15Co8Cu8Mn and 8Co8Cu8Mn catalysts were even weaker than those on the corresponding reduced catalysts, which implied that although some metallic Co particles would be converted to Co_2C species on these AC supported Co catalysts, small Co^0 particles can be maintained during reaction.

3.4 HR-TEM Observations

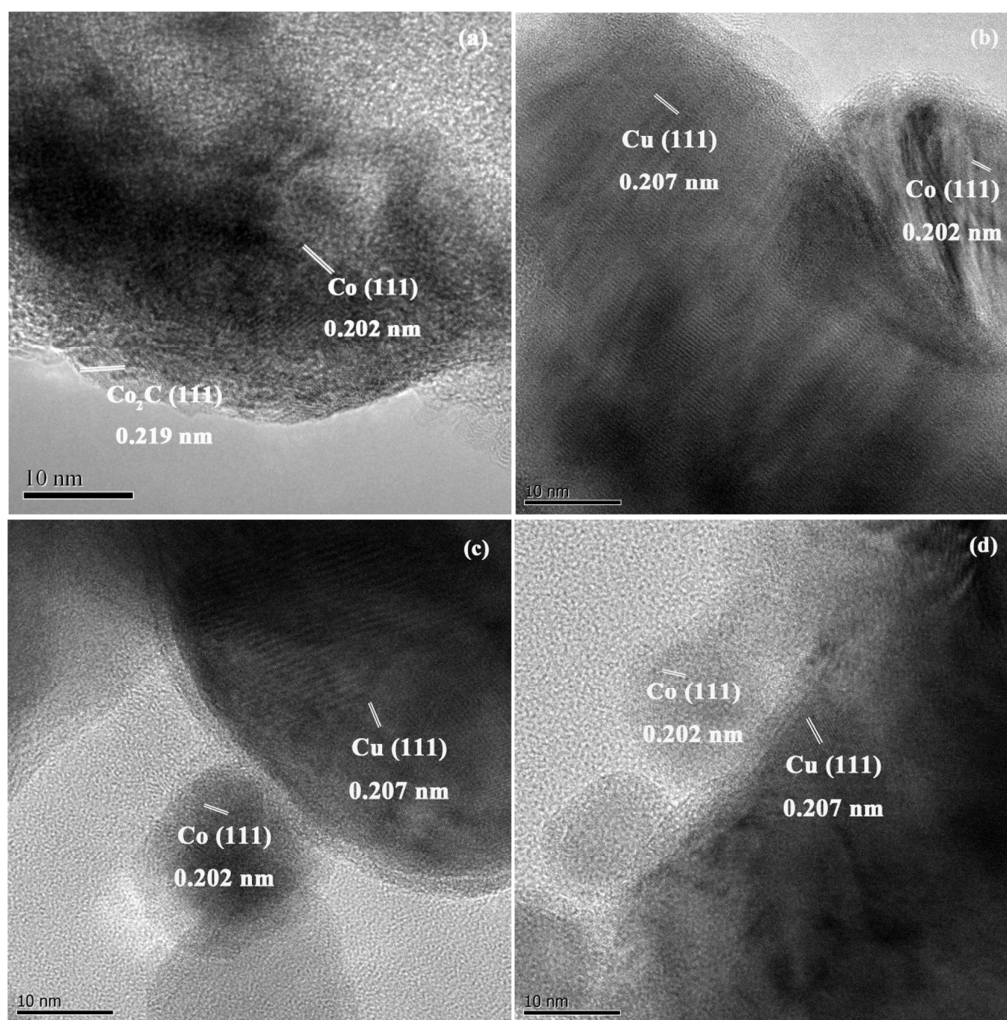


Fig. 5 HR-TEM images of the 15Co and the CoCuMn/AC catalysts after reaction and subsequent passivation: (a) 15Co; (b) 15Co4Cu4Mn; (c) 15Co8Cu8Mn; (d) 8Co8Cu8Mn.

We performed HR-TEM experiments to obtain structural information of the 15Co and the CoCuMn/AC catalysts after reaction and subsequent passivation. The HR-TEM image of the 15Co catalyst is shown in Fig. 5(a). The lattice spacings of 0.202 nm can be interpreted as the (111) plane of fcc metallic cobalt phases, while that of 0.219 nm can be assigned to the (111) plane of Co₂C phase, suggesting the co-existence of metallic Co and Co₂C species on the used 15Co catalyst which match well to the XRD results. Fig. 5 (b), (c) and (d) present the HR-TEM micrographs of the used 15Co4Cu4Mn, 15Co8Cu8Mn and 8Co8Cu8Mn catalysts, respectively. It can be clearly seen from each micrograph that there are small and nearly spherical nano-particles neighboring large nanocrystallines. The small particles with a measured lattice spacing of 0.202 nm can be attributed to the (111) plane of fcc Co, while the large nanocrystallines with the interplanar spacing of 0.207 nm can be ascribed to the (111) plane of Cu. It is usually difficult to identify and distinguish Co from Cu from the interplanar spacings of the (111) plane, because the values of the d spacings are very similar. However, the results of XRD characterization of the used 15Co4Cu4Mn, 15Co8Cu8Mn and 8Co8Cu8Mn catalysts are indicative of large Cu crystallites and small Co nano-particles, which reinforced the HR-TEM observations. No crystalline line corresponding to Co₂C was observed in these three figures, indicating the participation of Co₂C phases in such structure can be

excluded.

Now let us attempt to analyze the catalytic properties of the catalysts with the characterization results in more detail. It has been reported that Co_2C was responsible for the alcohol formation on Co/AC catalysts [10-12, 26], and thereby one can note that alcohols were produced on the 15Co catalyst in the presence of in situ formed Co_2C species. When the 15Co catalyst were added with 4% Cu and 4% Mn, the Co_2C formation was promoted as compared with the 15Co catalyst, and this effect was further enhanced when Cu and Mn content continued to increase. One can also note that the formation of metallic Cu phases followed the same trend as that of Co_2C , but only a gradual slow increase of alcohol selectivities was obtained. However, the alcohol selectivities were significantly enhanced when the Co loadings were decreased which resulted in a substantially reduced formation of Co_2C species but a considerably improved formation of metallic Cu phases on the 8Co8Cu8Mn catalyst. This suggested that although the Co_2C and metallic Cu phases, characteristic sites for alcohol formation, were tunable on Co/AC catalysts, Co prevailed to steer the products to hydrocarbons. Thus, it can be speculated that the ratio between alcohol and hydrocarbon formation sites plays fundamental role in controlling product selectivities. It is suggested in the literatures that the increase of Co_2C formation or $\text{Co}_2\text{C}/\text{Co}$ ratio on Co/AC catalysts could improve alcohol selectivities

[10,11]. However, we failed to increase alcohol selectivities by utilizing Co_2C active sites in the present case. Fortunately, one can clearly see that a proper Co-Cu composition is beneficial to improve alcohol selectivities. In fact, it has been widely accepted that an appropriate balance of Co-Cu composition has to be chosen for the synthesis of alcohols [22]. In addition, previous reports suggest that only the number of Co^0 that in-situ formed during reaction on Co/AC catalysts are responsible for the activity (CO conversion) [12,17], which is difficult to determine quantitatively and remain a task for future work. For this work, one can see from XRD results that the Co particle size decreased when taking into consideration the above-mentioned varying trend of Cu, Mn and Co content. Thus, we speculated that smaller Co particle probably contributed to more number of Co^0 which would result in increase of catalyst activity, although the contributions to Co^0 number from Co loading, Co reducibility, and Co_2C formation were different for all the catalysts. It is well known that the formation of alcohols needs a synergy between closely contacted metallic copper and cobalt species on CoCu bimetal catalysts [14,27]. Our HR-TEM observations concur with the literatures. More importantly, it can be clearly seen that large Cu particles are decorated by small Co nano-particles, which we propose that such structure was responsible for the preferential formation of C_{2+} alcohols.

We now turn to compare the catalytic performance of the

CoCuMn/AC catalysts with that of an AC supported CoCu bi-metal catalyst. This comparison is made in terms of activity, alcohol selectivity, and alcohol distribution for the 15Co4Cu4Mn catalyst and the 15Co4Cu catalyst. It can be seen from Table S1 that the performance of activity and alcohol selectivities of the binary catalyst is much lower than those of the 15Co4Cu4Mn catalyst, and even lower than those of the 15Co catalyst. It is also noteworthy that methanol formation is much higher than that of the 15Co4Cu4Mn catalyst, which can be explained if one remembers that Cu is a methanol producing site. Thus, it is obvious that the addition of Mn is beneficial for the catalytic performance in higher alcohol synthesis. XRD characterization of the used 15Co4Cu catalyst revealed the co-existence of Co, Cu and Co₂C phases (see Fig. S1), but it is notable that the intensities of peaks of Co₂C and Co components became the strongest and the widths of the peaks became the narrowest apparently, suggesting that severe carbidization and aggregation of Co particles occurred as compared with other catalysts. The decline of the reaction rate of Co catalysts is usually attributed to several mechanisms, such as sintering, catalyst poisoning, active metal re-oxidation, metal-support compound formation, and carbidization [28]. Our analysis suggested that the serious carbidization and sintering of Co particles on the 15Co4Cu catalyst might result in remarkably reduced Co⁰ number and thereby significantly decreased reaction rate of the 15Co4Cu catalyst. A careful

HR-TEM examination on the spent 15Co4Cu catalyst revealed that no structure containing closely contacted Co and Cu species similar to the cases of the CoCuMn/AC catalysts can be found. On Co-Cu type catalysts for alcohol synthesis, the intimate Co-Cu center is thought to be the active site for alcohol synthesis, on which Co functioning as CO dissociative activation and chain propagation site while Cu functioning as CO molecular activation and insertion site, the synergistic effect between Co and Cu is crucial to alcohol formation. It is speculated that the separation of Co and Cu phases might occur on the used 15Co4Cu catalyst, which would break the synergetic interaction between Co and Cu active sites [29], making Co easy to suppress alcohol formation. The interesting result regarding alcohol distribution is that the CoCuMn/AC catalysts favored the production of C₂₊ alcohols, with alcohols preferentially formed in the carbon number range of 2-5 and methanol formation severely suppressed. Many factors can be advanced to tune the shift in the product (hydrocarbon and/or alcohols) distribution of Co based catalysts for FT reaction, such as promoters [9,12,30], texture properties of support materials [31-33], reaction conditions [14,34], etc, however, studies on the product distribution over Co/AC catalyst systems are extremely scarce. From the literatures [12,17], we know that the texture properties of the AC support after the introduction of active components had little impact on catalyst performance. In light of the

report by Ying et al. [35], who well documented the influence of operation conditions on the Co/AC catalyst systems, we in fact tested the catalysts at the optimum reaction conditions in order to obtain the maximum selectivities towards alcohols. The situation is more complicated when promoters such Al, Si, and La are added to Co/AC catalysts [10,12,17]. As for the Mn additive, it is known that Mn usually provides a dispersion effect of active sites and/or a favorable production of olefins for Co-Cu type catalysts [7,36]. With the present work, there is no doubt that the addition of Mn species led to the formation of closely contacted Co and Cu phases with the micro-structure that small-sized Co particles were situated on the external surface of large Cu particles, which we suggested that such structure was responsible for the preferential formation of C₂₊ alcohols. For better understanding the mechanism for the influence of Mn species on the catalytic performance concerning activity, selectivity as well as product distribution of the CoCuMn/AC catalysts, further studies would be desirable.

4. Conclusions

A series of CuCoMn/AC catalysts were prepared and tested for FT reaction. It is found that the CoCuMn/AC catalysts exhibited good activity and selectivities to alcohols with substantially reduced methanol production but significant increased formation of C₂-C₅ alcohols. The enhanced activity (CO conversion) was attributable to the increase of Co⁰

number during reaction, whilst the improved alcohol selectivity was closely associated with the Cu/Co composition ratio. It is considered that the decoration of large Cu cluster with small Co nano-particle was responsible for the preferential production of C₂₊ alcohols. Future optimization of the active sites and catalyst structure are expected to result in additional improvements in catalytic performance.

References

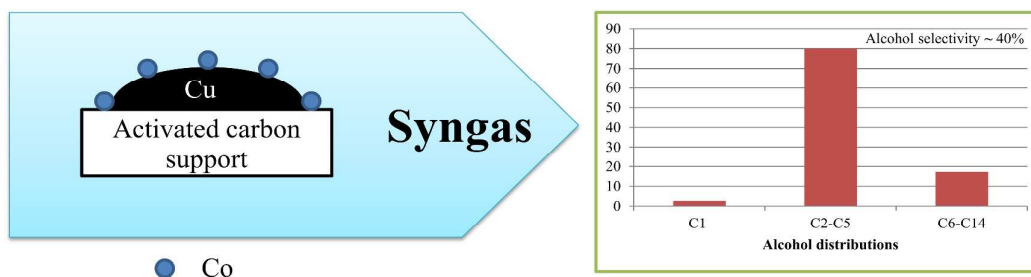
- [1] A. Y. Khodakov, W. Chu and P. Fongarland, *Chem. Rev.*, 2007, **107**, 1692.
- [2] E. de Smit and B. M. Weckhuysen, *Chem. Soc. Rev.*, 2008, **37**, 2758.
- [3] Q. H. Zhang, J. C. Kang and Y. Wang, *ChemCatChem*, 2010, **2**, 1030.
- [4] H. L. Li, S. G. Wang, F. X. Ling and J. L. Li, *J. Mol. Catal. A*, 2006, **244**, 33.
- [5] X. Yang, Y. Wei, Y. Su and L. Zhou, *Fuel Process. Technol.*, 2010, **91**, 1168.
- [6] P. Forzatti, E. Tronconi and I. Pasquon, *Catal. Rev. Sci. Eng.*, 1991, **33**, 109.
- [7] Y. Z. Xiang, V. Chitry, P. Liddicoat, P. Felfer, J. Cairney, S. Ringer and N. Kruse, *J. Am. Chem. Soc.*, 2013, **135**, 7114.
- [8] Y. Z. Xiang, V. Chitry and N. Kruse, *Catal. Lett.*, 2013, **143**, 936.
- [9] T. Ishida, T. Yanagihara, X. H. Liu, H. Ohashi, A. Hamasaki, T. Honma, H. Oji, T. Yokoyama and M. Tokunaga, *Appl. Catal. A*, 2013, **458**,

145.

- [10] G. P. Jiao, Y. J. Ding, H. J. Zhu, X. M. Li, J. W. Li, R. H. Lin, W. D. Dong, L. F. Gong, Y. P. Pei and Y. Lu, *Appl. Catal. A*, 2009, **364**, 137.
- [11] V. M. Lebarbier, D. H. Mei, D. H. Kim, A. Andersen, J. L. Male, J. E. Holladay, R. Rousseau and Y. Wang, *J. Phys. Chem. C*, 2011, **115**, 17440.
- [12] Y. P. Pei, Y. J. Ding, H. J. Zhu, J. Zang, X. G. Song, W. D. Dong, T. Wang and Y. Lu, *Catal. Lett.*, 2014, **144**, 1433.
- [13] Z. R. Li, Y. L. Fu, M. Jiang, T. D. Hu, T. Liu and Y. N. Xie, *J. Catal.*, 2001, **199**, 155.
- [14] X. D. Xu, E. B. M. F. Doesburg and J. J. F. Scholten, *Catal. Today*, 1987, **2**, 125.
- [15] H. Dlamini, T. Motjope, G. Joost, G. Stegelter and M. Mdleleni, *Catal. Lett.*, 2002, **78**, 201.
- [16] S. R. D. Migue, M. C. R. Martinez, E. L. Jablonski and J. L. G. Fierro, *J. Catal.*, 1999, **184**, 514.
- [17] Y. P. Pei, Y. J. Ding, H. J. Zhu and H. Du, *Chin. J. Catal.*, 2015, **36**, 355.
- [18] A. Griboval-Constant, A. Butel, V. V. Ordonsky, P. A. Chernavskii and A. Y. Khodakov, *Appl. Catal. A*, 2014, **481**, 116.
- [19] K. D. Jung and A. T. Bell, *J. Catal.*, 2000, **193**, 207.
- [20] J. Thiessen, A. Rose, J. Meyer, A. Jess and D. Curulla-Ferré, *Micropor. Mesopor. Mat.*, 2012, **164**, 199.

- [21] G. L. Bezemer, P. B. Radstake, U. Falke, H. Oosterbeek, H. P. C. E. Kuipers, A. J. van Dillen and K. P. de Jong, *J. Catal.*, 2006, **237**, 152.
- [22] N. D. Subramanian, G. Balaji, C. S. S. R. Kumar and J. J. Spivey, *Catal. Today*, 2009, **147**, 100.
- [23] Z. Q. Yang, C. Y. You and L. L. He, *J. Alloys Compd.*, 2006, **423**, 128.
- [24] J. Llorca, N. Homs, O. Rossell, M. Seco, J.-L. G. Fierro and P. R. de la Piscina, *J. Mol. Catal. A*, 1999, **149**, 225.
- [25] G. G. Volkova, T. M. Yurieva, L. M. Plyasova, M. I. Naumova and V. I. Zaikovskii, *J. Mol. Catal. A*, 2000, **158**, 389.
- [26] Y. P. Pei, J. X. Liu, Y. H. Zhao, Y. J. Ding, T. Liu, W. D. Dong, H. J. Zhu, H. Y. Su, Y. Li, J. L. Li and W. X. Li, *ACS Catal.*, 2015, **5**, 3620.
- [27] G. Prieto, S. Beijer, M. L. Smith, M. He, Y. Au, Z. Wang, D. A. Bruce, K. P. de Jong, J. J. Spivey and P. E. de Jongh, *Ange. Chem. Int. Ed.*, 2014, **53**, 6397.
- [28] M. Sadeqzadeh, S. Chambrey, J. P. Hong, P. Fongarland, F. Luck, D. Curulla-Ferré, D. Schweich, J. Bousquet and A. Y. Khodakov, *Ind. Eng. Chem. Res.*, 2014, **53**, 6913.
- [29] W. Gao, Y. F. Zhao, H. R. Chen, H. Chen, Y. W. Li, S. He, Y. K. Zhang, M. Wei, D. G. Evans and X. Duan, *Green Chem.*, 2015, **17**, 1525.
- [30] X. Dong, X. L. Liang, H. Y. Li, G. D. Lin, P. Zhang and H. B. Zhang, *Catal. Today*, 2009, **147**, 158.

- [31] V. R. Surisetty, A. K. Dalai and J. Kozinski, *Appl. Catal. A*, 2011, **393**, 50.
- [32] M. M. Lv, W. Xie, S. Sun, G. M. Wu, L. R. Zheng, S. Q. Chu, C. Gao and J. Bao, *Catal. Sci. Technol.*, 2015, **5**, 2925.
- [33] D. C. Song and J. L. Li, *J. Mol. Catal. A*, 2006, **247**, 206.
- [34] D. Vervloet, F. Kapteijn, J. Nijenhuis and J. R. van Ommen, *Catal. Sci. Technol.*, 2012, **2**, 1221.
- [35] W. X. Qian, H. T. Zhang, W. Y. Ying and D. Y. Fang, *J. Nat. Gas Chem.*, 2011, **20**, 389.
- [36] A Cosultchi, M. Pérez-Luna, J. A. Morales-Serna and M. Salmón, *Catal. Lett.*, 2012, **142**, 368.



Activated carbon supported CoCu catalysts with structures containing small-sized Co particles bordering large Cu particles favored formation of C₂+ alcohols.